

Melting, Reentrant Ordering and Peak Effect For Wigner Crystals with Quenched and Thermal Disorder

C. Reichhardt and C. J. O. Reichhardt
*Theoretical Division and Center for Nonlinear Studies,
 Los Alamos National Laboratory,
 Los Alamos, New Mexico 87545, USA*

(Dated: November 23, 2022)

We consider simulations of Wigner crystals interacting with random quenched disorder in the presence of thermal fluctuations. When quenched disorder is absent, there is a well defined melting temperature determined by the proliferation of topological defects, while for zero temperature, there is a critical quenched disorder strength above which topological defects proliferate. When both thermal and quenched disorder are present, these effects compete, and the thermal fluctuations can reduce the effectiveness of the quenched disorder, leading to a reentrant ordered phase in agreement with the predictions of Nelson [Phys. Rev. B 27, 2902 (1983)]. The onset of the reentrant phase can be deduced based on changes in the transport response, where the reentrant ordering appears as an increase in the mobility or the occurrence of a depinning transition. We also find that when the system is in the ordered state and thermally melts, there is an increase in the effective damping or pinning. This produces a drop in the electron mobility that is similar to the peak effect phenomenon found in superconducting vortices, where thermal effects soften the lattice or break down its elasticity, allowing the particles to better adjust their positions to take full advantage of the quenched disorder.

There is a wide class of systems of two-dimensional (2D) particle assemblies that form triangular crystalline phases, including vortices in thin film superconductors¹, colloidal particles²⁻⁴, dusty plasmas^{5,6}, magnetic skyrmions^{7,8}, active matter⁹, and electron solids or Wigner crystals^{10,11}. In the absence of quenched disorder, these systems exhibit a melting transition under increasing temperature that can be characterized by the proliferation of topological defects such as dislocations and disclinations^{3,12,13}. The melting transition in 2D systems has been intensely studied and can occur as a two step transition with an intermediate hexatic phase or as a single weakly first order phase transition^{12,14,15}. Even if a hexatic phase is present, the two steps of the transition can occur so close together that it becomes difficult to distinguish whether there are two separate phases in addition to the solid phase³.

Crystalline systems confined to 2D can also show order to disorder transitions as a function of increasing quenched disorder strength. At $T = 0$ there can be a critical disorder strength above which an amorphous phase appears^{16,17}. When there are both quenched disorder and thermal fluctuations, there can be a competition in which thermal fluctuations soften the interactions between particles but at the same time also reduce the effectiveness of the disordered substrate. Nelson¹⁸ proposed that for a 2D system with quenched disorder, thermal effects can wash out the quenched disorder, leading to a thermally induced reentrant ordering effect from a low temperature amorphous state to a crystal state as a function of increasing temperature. At still higher temperatures, the system thermally melts. In other studies, it was suggested that the quenched disorder always enhances the appearance of a disordered state, and that in-

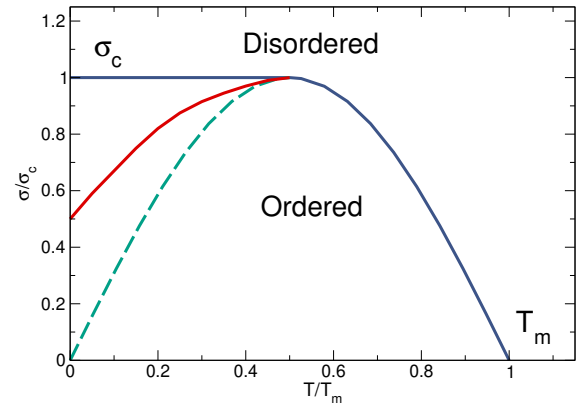


FIG. 1. Schematic phase diagram as a function of reduced quenched disorder strength σ/σ_c versus reduced temperature T/T_m for a 2D assembly of repulsive particles in the presence of quenched disorder. Here σ_c is the quenched disorder strength at the threshold for dislocation proliferation at $T = 0$, while T_m is the melting temperature at $\sigma = 0$. The green dashed line is the prediction from Nelson¹⁸ showing a reentrant disordered phase. The solid blue line is the prediction from Cha and Fertig¹⁶, and the solid red line is the result we find in this work.

roduction of quenched disorder monotonically decreases the temperature at which the transition from a disorder-induced amorphous state to a thermally reordered state occurs^{16,17,19}.

It is possible that the reentrant ordering proposed by Nelson¹⁸ may depend on the size scale and strength of

the quenched disorder pinning sites. For systems with long range particle-particle interactions but short range particle-pin interactions, reentrant ordering is possible when the pinning sites are sufficiently small. In Fig. 1 we show a schematic phase diagram as a function of reduced disorder strength σ/σ_c versus temperature T/T_m highlighting the ordered and disordered phases. When $\sigma = 0$, a melting transition occurs at T_m . The schematic does not distinguish whether there is also a hexatic phase, but simply indicates the point at which topological defects start to proliferate. At $T = 0$, for increasing σ there is a transition from a crystal to a disordered state at σ_c . On the right hand side of the figure, the solid line indicates that the critical value σ_c at which the system disorders decreases with increasing temperature. The three lines on the left hand side of the figure indicate different possible low temperature behaviors. The dashed line is the prediction from Nelson¹⁸, where the system is disordered at very low T but thermal effects wash out the effect of the disorder, permitting reordering to occur with increasing temperature. Cha and Fertig¹⁶ predicted the upper blue solid line, where the system remains ordered at low temperatures all the way up to a constant critical σ_c . The solid red line is what we observe in the present work, where disordering occurs even at $T = 0$ when σ is increased, but for $\sigma < \sigma_c$ there is a reentrant ordering with increasing temperature, so that the predictions of both Nelson and of Cha and Fertig occur. We also find that for finite σ , the thermally induced melting transition at higher temperatures is depressed in temperature. We note that in their simulation work, Cha and Fertig found that at $T = 0$ there is a critical disorder strength σ_c for the 2D crystal to disorder; however, they did not consider the effect of finite temperature to see whether there might still be a reentrant thermally reordered phase.

Another feature of 2D systems with quenched disorder is that the transport of the system should strongly depend on whether the particle arrangement is crystalline, disordered, or fluid^{17,20–24}. If the system is in a crystal state, there can still be a depinning threshold, but the depinning will be an elastic process in which particles keep their same neighbors^{17,20,23}. If the system is disordered or glassy, the depinning can be plastic where a portion of particles remain immobile while the other particles move, creating local tearing in the assembly^{17,20,22}. In the fluid phase, strong thermal hopping reduces the effects of the quenched disorder. For $T = 0$, the depinning threshold F_c shows a pronounced change across σ_c , where in general F_c rapidly increases with increasing σ once the system is on the disordered side of the transition where the depinning is plastic^{17,20,23}. Additionally, both the shape of the velocity-force curves and the fluctuations in the moving state show pronounced changes across the transition from elastic to plastic depinning, going from a single step depinning process on the elastic side to a multiple step process in the plastic phase^{17,20–23}. The jump up in pinning effectiveness upon crossing from elastic to plastic depinning has previously been argued

to be the cause of what is called the peak effect phenomenon observed in type-II superconductors^{25–37}. In the superconducting vortex system, the driving forces on the vortices arise from an applied current J , and the vortices depin above a critical current J_c . The peak effect occurs when, as a function of increasing temperature, J_c undergoes a rapid increase at a well defined temperature or magnetic field. If the vortices are already moving when the temperature is increased, there is a drop in their average velocity at the peak effect temperature. The apparent increase in the effectiveness of the pinning with increasing temperature is counterintuitive because it is more natural to expect that increasing the temperature would reduce the effectiveness of the pinning. In the peak effect regime, the thermal fluctuations are argued to reduce the elasticity of the vortex lattice (VL) or induce the formation of dislocations that strongly soften the VL, causing the VL to become amorphous and permitting individual vortices to easily adjust to the pinning landscape in order to become better pinned^{25,28,29}. As the temperature is increased further, the thermal fluctuations overwhelm the pinning energy and the vortices easily hop out of the pinning sites, causing a decrease in the critical current or equivalently an increase in the vortex velocity at fixed current. It is also possible to observe the peak effect as a function of increasing field, and in this case it is argued that changes in the magnetic penetration depth can reduce the strength of the vortex-vortex interactions and soften the VL. Various measures of the VL structure show that the peak effect is characterized by a transition from an ordered lattice to a disordered or amorphous state^{30,33,34}. The peak effect occurs in both 2D and three-dimensional (3D) systems, and the 3D peak effect is associated with first order characteristics and history dependence^{33,36}. The peak effect should be a general feature in any type of 2D elastic system coupled to quenched disorder where thermal effects can cause a softening of the lattice, leading to an increase in the depinning threshold or a drop in the velocity across the elastic to plastic transition.

Another system that forms a 2D crystal state that can be driven is electron solids or Wigner crystals^{38–47}. These systems usually contain some form of quenched disorder, and a variety of studies have revealed nonlinear transport and possible depinning thresholds^{40–43} associated with enhanced noise⁴⁵. Wigner crystals can also undergo melting transitions as a function of increasing temperature^{48–52}. There is a growing number of systems where Wigner crystals could be realized, including dichalcogenide monolayers⁵³, moiré heterostructures^{54,55}, bilayer systems⁵⁶, and Wigner crystals at zero field⁵⁷, while new advances in materials preparation point to a variety of future experiments that could be done in which the competition between quenched disorder and thermal effects could be studied¹¹. Unlike colloidal assemblies or superconducting vortices, imaging experiments for Wigner systems are difficult, so the existence of order to disorder or melting transitions must be determined

on the basis of some type of response or transport experiments. An open question is what the Wigner crystal phase diagram is as a function of quenched disorder and temperature, as illustrated schematically in Fig. 1, and whether the different phases can be deduced from transport measures. Another question is whether Wigner crystals can also exhibit a peak effect or an increase in the effectiveness of the pinning as a function of increasing temperature similar to what is found in superconducting vortex systems across a thermally induced disordering transition.

In this work we perform simulations of a 2D localized electron system in the presence of quenched disorder σ and thermal disorder T . At $\sigma = 0$, there is a well defined melting temperature T_m characterized by a proliferation of topological defects, while for $T = 0$ there is a well defined critical quenched disorder strength σ_c above which topological defects proliferate. We map out the phase diagram as a function of σ versus T/T_m and find that when $\sigma < \sigma_c$, an increase in T can cause the system to thermally order as predicted by Nelson¹⁸. Additionally, when σ is finite, thermal disordering occurs at temperatures lower than T_m . For sufficiently large σ , the system is always disordered. We show that the ordered and disordered phases can be detected using transport signatures, where we apply a finite driving force and measure the changes in the average velocity. When $\sigma < \sigma_c$, the system forms a disordered pinned state at low temperatures, but at the reentrant ordering transition, a lattice with elastic behavior emerges and the depinning threshold is strongly reduced, leading to a finite velocity of the Wigner crystal. At higher temperatures where the system thermally melts, under driving the velocity drops as a function of increasing temperature in superconducting vortex systems^{25–36}. The peak effect we observe only occurs for $T/T_m < 1.0$. We show that reentrance in the phase diagram occurs both as a function of increasing disorder strength for fixed disorder density and as a function of increasing disorder density for fixed disorder strength, and that the peak effect remains robust for different values of the drive.

I. SIMULATION AND SYSTEM

We consider a 2D system with periodic boundary conditions in the x and y directions containing N_e localized electrons at an electron density of $n = N_e/L^2$, where the system is of size $L \times L$. Throughout this work we use $n = 0.44$, $L = 36$, and $N_e = 572$. The system also contains N_p localized pinning sites of density $n_p = N_p/L^2$. The initial electron configuration is obtained via simulated annealing, similar to what was done in previous simulations of Wigner crystals in the presence

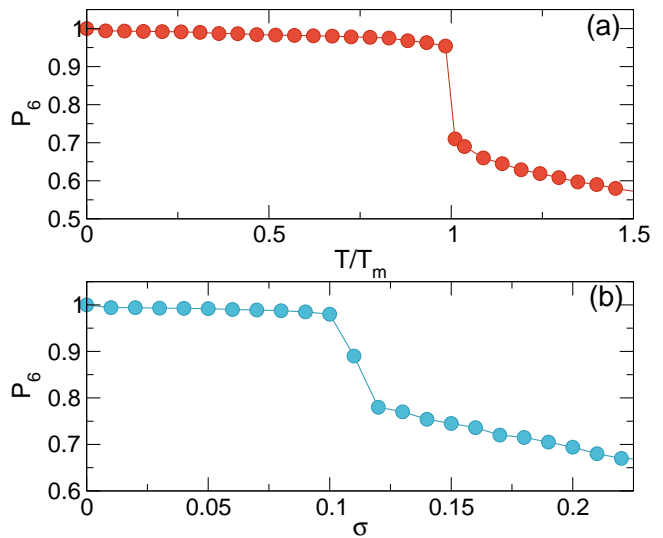


FIG. 2. (a) The fraction of sixfold coordinated electrons P_6 vs reduced temperature T/T_m for a system with no quenched disorder, $\sigma = 0$. There is a well defined melting temperature T_m indicated by the drop in P_6 . (b) P_6 vs disorder strength σ in a system with pinning density $n_p = 0.25$ and zero temperature, $T/T_m = 0$. There is a well defined value of σ , σ_c , at which topological defects begin to proliferate, leading to a drop in P_6 .

of disorder^{58–61}. The equation of motion for electron i in the Wigner crystal is

$$\alpha_d \mathbf{v}_i = \sum_j^N \nabla U(r_{ij}) + \mathbf{F}_p + \mathbf{F}_i^T + \mathbf{F}_D. \quad (1)$$

The damping term is α_d and the electron-electron repulsive interaction potential is $U(r_{ij}) = q/r_{ij}$, where q is the electron charge, \mathbf{r}_i and \mathbf{r}_j are the positions of electrons i and j , and $r_{ij} = |\mathbf{r}_i - \mathbf{r}_j|$. Since the interactions are of long range, we employ a real space version of a modified Ewald summation technique called the Lekner method as in previous work^{62,63}. The pinning force \mathbf{F}_p is modeled as arising from randomly placed short range parabolic traps of radius $r_p = 0.35$. The thermal fluctuations \mathbf{F}^T are represented by Langevin kicks with the properties $\langle \mathbf{F}_i^T \rangle = 0$ and $\langle \mathbf{F}_i^T(t) \mathbf{F}_j^T(t') \rangle = 2k_B T \delta_{ij} \delta(t - t')$. We also consider the effect of an applied driving force $\mathbf{F}_D = F_D \hat{\mathbf{x}}$, which could come from an applied voltage. We measure the average velocity per particle, $\langle V \rangle = \sum_i^{N_e} \mathbf{v}_i \cdot \hat{\mathbf{x}}$, allowing us to construct the equivalent of an experimental current-voltage curve. The simulation method we employ for the pinning and dynamics of Wigner crystals was used previously to examine nonlinear velocity-force curves⁵⁸, noise⁵⁹, and depinning thresholds^{61,64}. If the electrons are subjected to a magnetic field \mathbf{B} , there can be an additional force term $q\mathbf{B} \times \mathbf{v}_i$ that can generate a Hall angle for the electron motion⁶⁰; however, in general this term is small and we will not consider it in this work.

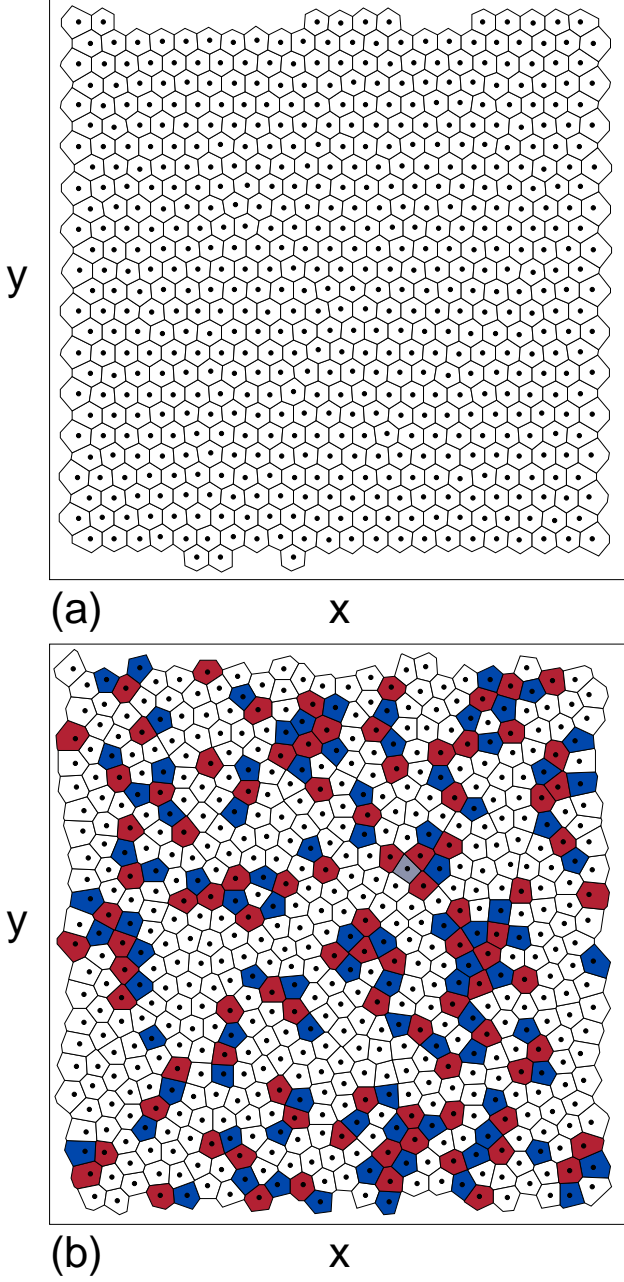


FIG. 3. Voronoi construction of the electron positions for the system in Fig. 2(a) with no quenched disorder, $\sigma = 0$. White polygons are sixfold coordinated, blue are fivefold coordinated, red are sevenfold coordinated, and gray are fourfold coordinated. (a) At $T/T_m = 0.52$ the lattice is triangular. (b) At $T/T_m = 1.09$, numerous topological defects have appeared and the system is in a liquid state.

II. RESULTS

We first study a sample containing no quenched disorder. To characterize the system we use the fraction of sixfold coordinated electrons, $P_6 = N_e^{-1} \sum_i \delta(z_i - 6)$, where the coordination number z_i of electron i is obtained

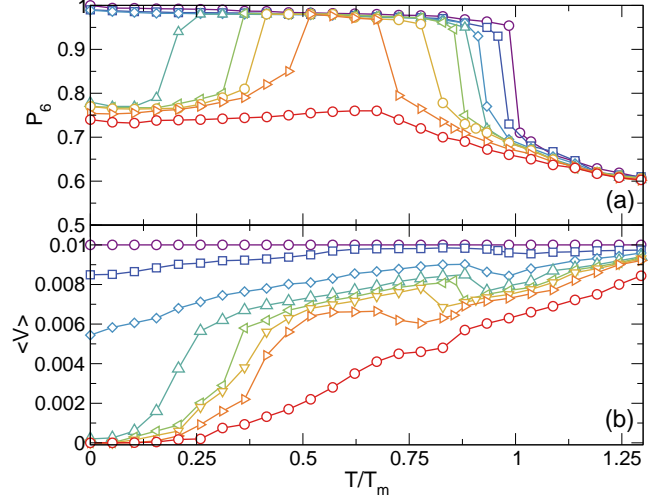


FIG. 4. (a) P_6 vs T/T_m for the system in Fig. 2 with $n_p = 0.25$ at $\sigma = 0.0, 0.06, 0.1, 0.12, 0.13, 0.135, 0.14$, and 0.16 , from top to bottom. For $\sigma = 0.0, 0.06$, and 0.1 , there is no reentrant ordering, but for $\sigma = 0.12, 0.13, 0.135$, and 0.14 , there is reentrant ordering with increasing temperature. (b) The corresponding velocity $\langle V \rangle$ vs T/T_m at $F_D = 0.01$. The velocities are low in the disordered regime at lower T/T_m , but increase at the reentrant ordering transition. In addition, at the thermal melting transition there is a drop in $\langle V \rangle$ similar to the peak effect phenomenon found for superconducting vortices.

using a Voronoi construction. For a triangular lattice of electrons, $P_6 = 1.0$. In Fig. 2(a) we plot P_6 versus T/T_m , where the melting temperature T_m is defined to occur at the point where P_6 shows a rapid drop. Figure 2(a) indicates that the melting temperature is well defined. We plot the Voronoi construction for the electron positions at $T/T_m = 0.52$ in Fig. 3(a), where the lattice is ordered, and at $T/T_m = 1.09$ in Fig. 3(b), where numerous topological defects have appeared. In Fig. 2(b) we show P_6 versus the maximum disorder strength σ in a sample with a pinning density of $n_p = 0.25$ at zero temperature, $T = 0$. There is a well defined disorder strength $\sigma_c \approx 0.105$ above which a proliferation of topological defects occurs.

We next perform a series of simulations at different combinations of σ and T for the system from Fig. 2 with $n_p = 0.25$. In Fig. 4(a) we plot P_6 versus T/T_m at $\sigma = 0, 0.06, 0.1, 0.12, 0.13, 0.135, 0.14$, and 0.16 , where T_m is defined to be the temperature at which melting occurs for $\sigma = 0$. For $\sigma = 0.0, 0.06$, and 0.1 , the system starts off ordered at low T/T_m and remains ordered until it melts near $T/T_m = 1$. The drop in P_6 associated with melting shifts to lower values of T/T_m as σ increases. For $\sigma = 0.12, 0.13, 0.135$, and 0.14 , all of which are above the value of $\sigma = 0.105$ for which the system disorders at $T = 0$ in Fig. 2(b), the system is disordered at low temperature. As T/T_m increases, there is a critical temperature at which P_6 increases back to a value near $P_6 = 1$, indicating that the system has ordered under increasing

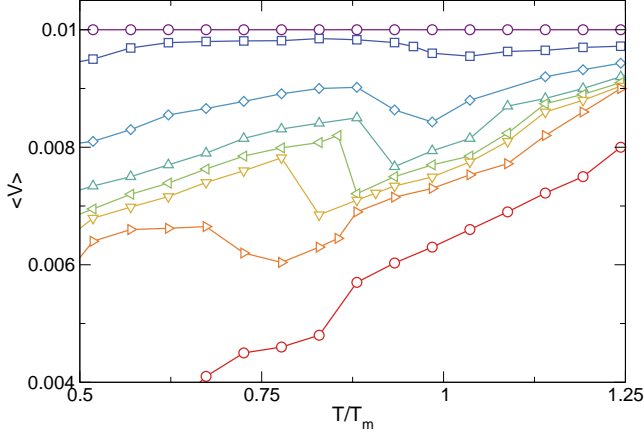


FIG. 5. A blowup of the plot of $\langle V \rangle$ vs T/T_m in Fig. 4(b) for the system in Fig. 2 with $n_p = 0.25$ at $\sigma = 0.0, 0.06, 0.1, 0.12, 0.13, 0.135, 0.14$, and 0.16 , from top to bottom, showing that the velocity drops across the thermal disordering transition.

temperature. The temperature at which this reentrant ordering occurs shifts to higher T/T_m with increasing σ , while the thermal disordering temperature drops to lower T/T_m as σ becomes larger, so for $\sigma = 0.14$ there is only a narrow window, $0.5 < T/T_m < 0.75$, where the system is ordered. For $\sigma = 0.16$, the system is disordered at all temperatures.

In Fig. 4(b) we plot $\langle V \rangle$ versus T/T_m for the same system in Fig. 4(a) where we have added a driving force with $F_D = 0.01$. Under this drive, the $\sigma = 0$ system has $\langle V \rangle = 0.01$ for all values of T/T_m . When $\sigma = 0.06$ or 0.1 , $\langle V \rangle$ starts off at a finite value and increases with increasing T/T_m ; however, for $\sigma > 0.1$, at low temperatures where P_6 is low, $\langle V \rangle = 0$. This indicates that the system is easily pinned in the low temperature disordered phase; however, when the system reaches the reentrant ordered state, it forms an elastic lattice that is less well pinned, leading to an increase in $\langle V \rangle$. Another interesting effect is that at the thermal melting transition, the drop in P_6 is also correlated with a drop in $\langle V \rangle$, indicating that the effectiveness of the pinning increases at the thermally induced disordering transition. This behavior is very similar to the peak effect phenomenon, where at a finite drive the average superconducting vortex velocity can show a drop with increasing temperature when the system thermally disorders. In the vortex case, it has been argued that the disordered state is softer and can therefore better adapt to the pinning landscape. Figure 4(b) shows that at higher temperatures where the thermal effects start to dominate, the velocity increases with increasing T/T_m . For $\sigma = 0.06$ there is only a weak dip in $\langle V \rangle$ at the thermal disordering temperature, and at $\sigma = 0.16$, there is no dip in the velocity since the system is always disordered.

In Fig. 5 we show a blowup of the $\langle V \rangle$ versus T/T_m plot from Fig. 4(b) in order to highlight the drop in $\langle V \rangle$ across the thermal melting transition. In general, the

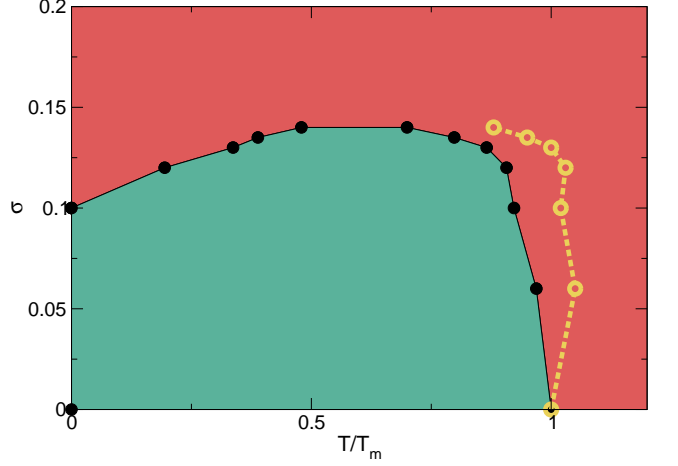


FIG. 6. Phase diagram as a function of pinning strength σ vs reduced temperature T/T_m constructed from the features in Fig. 4 for a system with $n_p = 0.25$. Green indicates the ordered regime and red indicates the disordered regime. Reentrant ordering occurs for $0.1 < \sigma < 0.14$. The peak effect appears between the disordering transition and the thermal melting regime, and the dashed line indicates the end of the peak effect window.

drop in velocity only appears at $T/T_m < 1.0$ and shifts to lower values of T/T_m as the pinning strength σ increases. This result indicates that both the reentrant ordering transition and the thermal melting can be detected using changes in the transport measures.

Using the features in Fig. 4, in Fig. 6 we construct a phase diagram as a function of σ versus T/T_m showing the ordered and disordered regimes. Reentrant ordering occurs for $0.1 < \sigma < 0.14$, and the thermally induced disordering transition drops further below $T/T_m = 1.0$ with increasing σ . The phase diagram includes the reentrant ordering feature predicted by Nelson¹⁸ as well as a finite value of σ_c at $T = 0$ as proposed by Cha and Fertig¹⁶. For $\sigma > 0.14$, the system is always disordered. The dashed line indicates the upper end of the region in which there is a velocity reduction associated with the peak effect. This line is determined by the point at which $\langle V \rangle$ reaches 75% of $\langle V_d \rangle$, where $\langle V_d \rangle$ is the value of $\langle V \rangle$ just before the velocity dip begins as a function of increasing T/T_m . We note that additional lines could be drawn in the disordered regime to differentiate between a low temperature glassy or pinned phase and a higher temperature fluctuating fluid phase.

In Fig. 7(a) we plot P_6 versus T/T_m for the system in Fig. 4 at a fixed $\sigma = 0.12$ for varied pinning densities of $n_p = 0, 0.15, 0.25, 0.35, 0.45$ and 0.55 . For $n_p = 0$ and 0.15 there is no disordered phase at low T/T_m ; however, for $0.25 \leq n_p \leq 0.45$, there is a regime of reentrant ordering. For $n_p = 0.55$, the system is disordered for all values of T/T_m . Figure 7(b) shows the corresponding $\langle V \rangle$ versus T/T_m curves. The drop in $\langle V \rangle$ at the thermal ordering transition indicates that the same peak effect

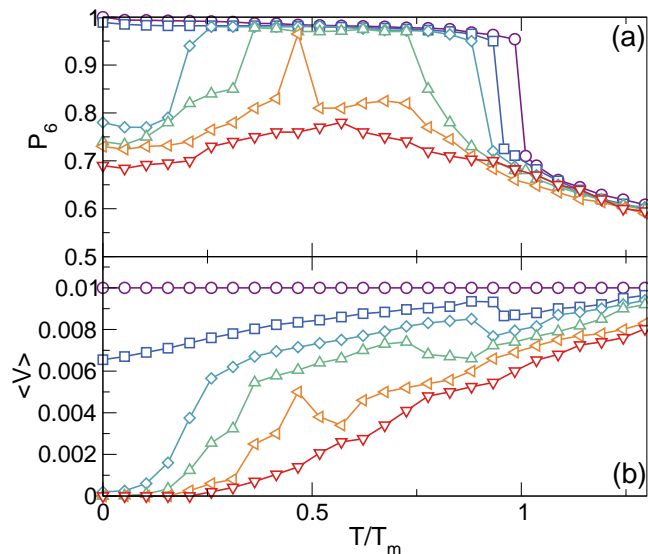


FIG. 7. (a) P_6 vs T/T_m for the system in Fig. 4 at fixed $\sigma = 0.12$ for $n_p = 0, 0.15, 0.25, 0.35, 0.45$, and 0.55 , from top to bottom. (b) The corresponding $\langle V \rangle$ vs T/T_m under a drive of $F_D = 0.01$ showing a drop in velocity across the thermal melting transition.

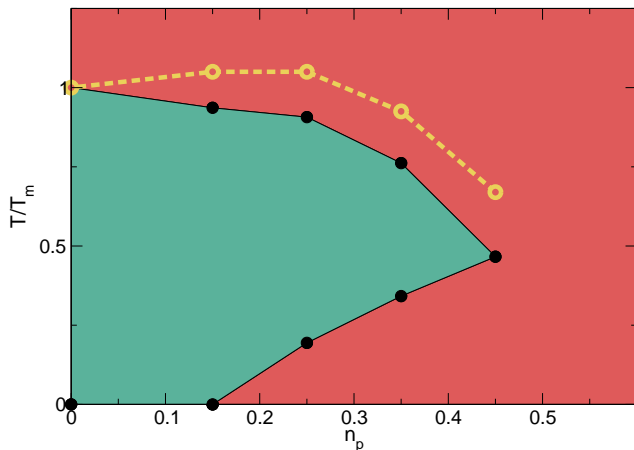


FIG. 8. Phase diagram as a function of reduced temperature T/T_m vs pinning density n_p constructed from the features in Fig. 7 for a system with $\sigma = 0.12$. Green indicates the ordered regime and red indicates the disordered regime. Reentrant ordering occurs for $0.15 < n_p < 0.45$. The dashed line indicates the end of the peak effect window where the velocity drop is lost.

appears that was found for varied disorder strengths. For $n_p = 0.55$, $\langle V \rangle$ monotonically increases with increasing T/T_m .

In Fig. 8 we show a phase diagram of the ordered and disordered states as a function of T/T_m versus pinning density n_p constructed using the features in Fig. 7. The same reentrant ordering phase appears that was found in Fig. 6 at constant pinning density for changing pinning strength. The dashed line indicates where the drop in

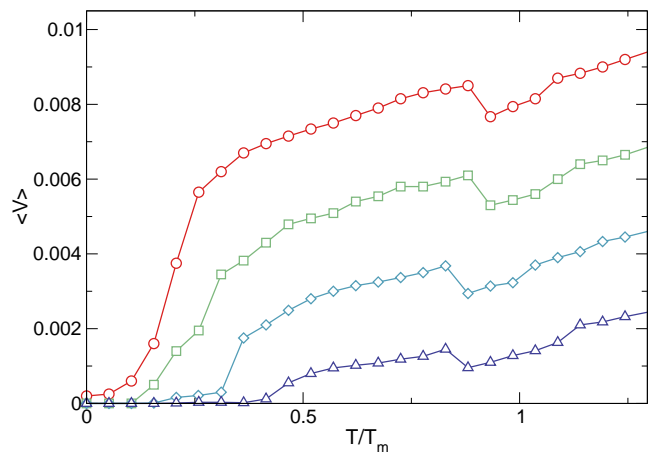


FIG. 9. $\langle V \rangle$ vs T/T_m curves for a system with $\sigma = 0.12$ and $n_p = 0.25$ at $F_D = 0.01, 0.0075, 0.005$, and 0.0025 , from top to bottom.

velocity associated with peak effect is lost.

We have also tested how robust the peak effect phenomenon is for varied driving force F_D . In Fig. 9 we plot $\langle V \rangle$ versus T/T_m for a system with $n_p = 0.25$ and $\sigma = 0.12$ at $F_D = 0.01, 0.0075, 0.005$, and 0.0025 . As F_D decreases, at low temperatures there is an extended window where the system is pinned, while at higher temperatures the peak effect region remains robust. The thermal melting transition shifts to slightly lower values of T/T_m with decreasing driving force. This result suggests that if F_D is low enough, the system could show a reentrant pinning near the thermal disordering transition.

III. SUMMARY

We have investigated the quenched disorder versus temperature phase diagram for a 2D Wigner crystal system. For zero quenched disorder, there is a well defined melting temperature that is characterized by the proliferation of topological defects. For zero temperature there is also a well defined quenched disorder strength at which the system becomes disordered. The phase diagram shows that when the disorder strength is larger than the value at which the zero temperature system becomes disordered, as the temperature is increased the system can show a thermally induced or reentrant ordering transition when the thermal fluctuations become strong enough to overwhelm the effect of the quenched disorder without melting the lattice. At higher temperatures, introduction of quenched disorder reduces the thermal disordering temperature of the system, while for strong enough quenched disorder the system is always disordered. The phase diagrams we obtain show both the reentrant ordering feature predicted by Nelson for 2D systems with quenched and thermal disorder as well as a well defined quenched disorder strength where the

electrons disorder at zero temperature, as predicted by Cha and Fertig. We also show that these phases can be observed through features in the transport curves, where the effectiveness of the pinning strongly drops at the reentrant ordering transition as the system goes from plastic behavior to elastic behavior. In the presence of quenched disorder, the thermal disordering transition is associated with a drop in the average electron velocity, similar to the peak effect phenomenon found in superconducting vortex systems. The drop occurs when thermal fluctuations break down the elasticity of the crystal and allow the electrons to adjust more easily to the pinning substrate. At higher temperatures, the velocity goes back up again when the electrons begin to hop readily out of the pinning barriers. We show that these effects are robust for a range of pinning strengths, densities, and drives. Our predic-

tions could be tested by examining transport signatures in Wigner crystals where both thermal and quenched disorder effects arise. Our results should be general to the broader class of 2D systems with quenched disorder.

ACKNOWLEDGMENTS

We gratefully acknowledge the support of the U.S. Department of Energy through the LANL/LDRD program for this work. This work was supported by the US Department of Energy through the Los Alamos National Laboratory. Los Alamos National Laboratory is operated by Triad National Security, LLC, for the National Nuclear Security Administration of the U. S. Department of Energy (Contract No. 892333218NCA000001).

- ¹ I. Guillamon, H. Suderow, A. Fernandez-Pacheco, J. Sese, R. Cordoba, J. M. De Teresa, M. R. Ibarra, and S. Vieira, “Direct observation of melting in a two-dimensional superconducting vortex lattice,” *Nature Phys.* **5**, 651–655 (2009).
- ² C. A. Murray and D. H. Van Winkle, “Experimental observation of two-stage melting in a classical two-dimensional screened Coulomb system,” *Phys. Rev. Lett.* **58**, 1200–1203 (1987).
- ³ K. Zahn, R. Lenke, and G. Maret, “Two-stage melting of paramagnetic colloidal crystals in two dimensions,” *Phys. Rev. Lett.* **82**, 2721–2724 (1999).
- ⁴ C. Reichhardt and C. J. Olson Reichhardt, “Fluctuating topological defects in 2D liquids: Heterogeneous motion and noise,” *Phys. Rev. Lett.* **90**, 095504 (2003).
- ⁵ H. Thomas, G. E. Morfill, V. Demmel, J. Goree, B. Feuerbacher, and D. Möhlmann, “Plasma crystal: Coulomb crystallization in a dusty plasma,” *Phys. Rev. Lett.* **73**, 652–655 (1994).
- ⁶ C.-H. Chiang and L. I, “Cooperative particle motions and dynamical behaviors of free dislocations in strongly coupled quasi-2D dusty plasmas,” *Phys. Rev. Lett.* **77**, 647–650 (1996).
- ⁷ P. Huang, T. Schonenberger, M. Cantoni, L. Heinen, A. Magrez, A. Rosch, F. Carbone, and H. M. Rønnow, “Melting of a skyrmion lattice to a skyrmion liquid via a hexatic phase,” *Nature Nanotechnol.* **15**, 761 (2020).
- ⁸ J. Zázvorka, F. Dittrich, Y. Ge, N. Kerber, K. Raab, T. Winkler, K. Litzius, M. Veis, P. Virnau, and M. Kläui, “Skyrmion lattice phases in thin film multilayer,” *Adv. Funct. Mater.* **30**, 2004037 (2020).
- ⁹ P. Digregorio, D. Levis, L. F. Cugliandolo, G. Gonnella, and I. Pagonabarraga, “Unified analysis of topological defects in 2D systems of active and passive disks,” *Soft Matter* **18**, 566–591 (2022).
- ¹⁰ P. Monceau, “Electronic crystals: an experimental overview,” *Adv. Phys.* **61**, 325–581 (2012).
- ¹¹ M. Shayegan, “Wigner crystals in flat band 2D electron systems,” *Nature Rev. Phys.* **4**, 212–213 (2022).
- ¹² K. J. Strandburg, “Two-dimensional melting,” *Rev. Mod. Phys.* **60**, 161–207 (1988).
- ¹³ H. H. von Grünberg, P. Keim, K. Zahn, and G. Maret, “Elastic behavior of a two-dimensional crystal near melting,” *Phys. Rev. Lett.* **93**, 255703 (2004).
- ¹⁴ A. H. Marcus and S. A. Rice, “Observations of first-order liquid-to-hexatic and hexatic-to-solid phase transitions in a confined colloid suspension,” *Phys. Rev. Lett.* **77**, 2577–2580 (1996).
- ¹⁵ D. Du, M. Doxastakis, E. Hilou, and S. L. Biswal, “Two-dimensional melting of colloids with long-range attractive interactions,” *Soft Matter* **13**, 1548–1553 (2017).
- ¹⁶ M.-C. Cha and H. A. Fertig, “Disorder-induced phase transitions in two-dimensional crystals,” *Phys. Rev. Lett.* **74**, 4867–4870 (1995).
- ¹⁷ C. Reichhardt and C. J. Olson Reichhardt, “Depinning and nonequilibrium dynamic phases of particle assemblies driven over random and ordered substrates: a review,” *Rep. Prog. Phys.* **80**, 026501 (2017).
- ¹⁸ D. R. Nelson, “Reentrant melting in solid films with quenched random impurities,” *Phys. Rev. B* **27**, 2902–2914 (1983).
- ¹⁹ S. Deutschländer, T. Horn, H. Löwen, G. Maret, and P. Keim, “Two-dimensional melting under quenched disorder,” *Phys. Rev. Lett.* **111**, 098301 (2013).
- ²⁰ C. Reichhardt and C. J. Olson, “Colloidal dynamics on disordered substrates,” *Phys. Rev. Lett.* **89**, 078301 (2002).
- ²¹ A. Pertsinidis and X. S. Ling, “Statics and dynamics of 2D colloidal crystals in a random pinning potential,” *Phys. Rev. Lett.* **100**, 028303 (2008).
- ²² Y. Fily, E. Olive, N. Di Scala, and J. C. Soret, “Critical behavior of plastic depinning of vortex lattices in two dimensions: Molecular dynamics simulations,” *Phys. Rev. B* **82**, 134519 (2010).
- ²³ N. Di Scala, E. Olive, Y. Lansac, Y. Fily, and J. C. Soret, “The elastic depinning transition of vortex lattices in two dimensions,” *New J. Phys.* **14**, 123027 (2012).
- ²⁴ C. Reichhardt, D. Ray, and C. J. Olson Reichhardt, “Collective transport properties of driven skyrmions with random disorder,” *Phys. Rev. Lett.* **114**, 217202 (2015).
- ²⁵ A. B. Pippard, “A possible mechanism for peak effect in type 2 superconductors,” *Phil. Mag.* **19**, 217 (1969).
- ²⁶ P. H. Kes and C. C. Tsuei, “Two-dimensional collective flux pinning, defects, and structural re-

- laxation in amorphous superconducting films,” *Phys. Rev. B* **28**, 5126–5139 (1983).
- 27 R. Wördenweber, P. H. Kes, and C. C. Tsuei, “Peak and history effects in two-dimensional collective flux pinning,” *Phys. Rev. B* **33**, 3172–3180 (1986).
 - 28 S. Bhattacharya and M. J. Higgins, “Dynamics of a disordered flux line lattice,” *Phys. Rev. Lett.* **70**, 2617–2620 (1993).
 - 29 W. K. Kwok, J. A. Fendrich, C. J. van der Beek, and G. W. Crabtree, “Peak effect as a precursor to vortex lattice melting in single crystal $\text{YBa}_2\text{Cu}_3\text{O}_{7-\delta}$,” *Phys. Rev. Lett.* **73**, 2614–2617 (1994).
 - 30 P. L. Gammel, U. Yaron, A. P. Ramirez, D. J. Bishop, A. M. Chang, R. Ruel, L. N. Pfeiffer, E. Bucher, G. D’Anna, D. A. Huse, K. Mortensen, M. R. Eskildsen, and P. H. Kes, “Structure and correlations of the flux line lattice in crystalline Nb through the peak effect,” *Phys. Rev. Lett.* **80**, 833–836 (1998).
 - 31 S. S. Banerjee, N. G. Patil, S. Ramakrishnan, A. K. Grover, S. Bhattacharya, P. K. Mishra, G. Ravikumar, T. V. Chandrasekhar Rao, V. C. Sahni, M. J. Higgins, C. V. Tomy, G. Balakrishnan, and D. Mck. Paul, “Disorder, metastability, and history dependence in transformations of a vortex lattice,” *Phys. Rev. B* **59**, 6043–6046 (1999).
 - 32 Y. Paltiel, E. Zeldov, Y. N. Myasoedov, H. Shtrikman, S. Bhattacharya, M. J. Higgins, Z. L. Xiao, E. Y. Andrei, P. L. Gammel, and D. J. Bishop, “Dynamic instabilities and memory effects in vortex matter,” *Nature (London)* **403**, 398–401 (2000).
 - 33 X. S. Ling, S. R. Park, B. A. McClain, S. M. Choi, D. C. Dender, and J. W. Lynn, “Superheating and supercooling of vortex matter in a Nb single crystal: Direct evidence for a phase transition at the peak effect from neutron diffraction,” *Phys. Rev. Lett.* **86**, 712–715 (2001).
 - 34 A. M. Troyanovskii, M. van Hecke, N. Saha, J. Aarts, and P. H. Kes, “STM imaging of flux line arrangements in the peak effect regime,” *Phys. Rev. Lett.* **89**, 147006 (2002).
 - 35 M. Hilke, S. Reid, R. Gagnon, and Z. Altounian, “Peak effect and the phase diagram of moving vortices in $\text{Fe}_x\text{Ni}_{1-x}\text{Zr}_2$ superconducting glasses,” *Phys. Rev. Lett.* **91**, 127004 (2003).
 - 36 G. Pasquini, D. Pérez Daroca, C. Chliotte, G. S. Lozano, and V. Bekeris, “Ordered, disordered, and co-existent stable vortex lattices in NbSe_2 single crystals,” *Phys. Rev. Lett.* **100**, 247003 (2008).
 - 37 S. Okuma, K. Kashi, Y. Suzuki, and N. Kokubo, “Order-disorder transition of vortex matter in $\text{a-Mo}_x\text{Ge}_{1-x}$ films probed by noise,” *Phys. Rev. B* **77**, 212505 (2008).
 - 38 E. Wigner, “On the interaction of electrons in metals,” *Phys. Rev.* **46**, 1002–1011 (1934).
 - 39 E. Y. Andrei, G. Deville, D. C. Glatli, F. I. B. Williams, E. Paris, and B. Etienne, “Observation of a magnetically induced Wigner solid,” *Phys. Rev. Lett.* **60**, 2765–2768 (1988).
 - 40 V. J. Goldman, M. Santos, M. Shayegan, and J. E. Cunningham, “Evidence for two-dimensional quantum Wigner crystal,” *Phys. Rev. Lett.* **65**, 2189–2192 (1990).
 - 41 H. W. Jiang, H. L. Stormer, D. C. Tsui, L. N. Pfeiffer, and K. W. West, “Magnetotransport studies of the insulating phase around $\nu=1/5$ Landau-level filling,” *Phys. Rev. B* **44**, 8107–8114 (1991).
 - 42 F. I. B. Williams, P. A. Wright, R. G. Clark, E. Y. Andrei, G. Deville, D. C. Glatli, O. Probst, B. Etienne, C. Dorin, C. T. Foxon, and J. J. Harris, “Conduction threshold and pinning frequency of magnetically induced Wigner solid,” *Phys. Rev. Lett.* **66**, 3285–3288 (1991).
 - 43 G. Piacente and F. M. Peeters, “Pinning and depinning of a classic quasi-one-dimensional Wigner crystal in the presence of a constriction,” *Phys. Rev. B* **72**, 205208 (2005).
 - 44 J. Jang, B. M. Hunt, L. N. Pfeiffer, K. W. West, and R. C. Ashoori, “Sharp tunneling resonance from the vibrations of an electronic Wigner crystal,” *Nature Phys.* **13**, 340–344 (2017).
 - 45 P. Brussarski, S. Li, S. V. Kravchenko, A. A. Shashkin, and M. P. Sarachik, “Transport evidence for a sliding two-dimensional quantum electron solid,” *Nature Commun.* **9**, 3803 (2018).
 - 46 A. T. Hatke, H. Deng, Y. Liu, L. W. Engel, L. N. Pfeiffer, K. W. West, K. W. Baldwin, and M. Shayegan, “Wigner solid pinning modes tuned by fractional quantum Hall states of a nearby layer,” *Sci. Adv.* **5**, eaao2848 (2019).
 - 47 Md. S. Hossain, M. K. Ma, K. A. Villegas-Rosales, Y. J. Chung, L. N. Pfeiffer, K. W. West, K. W. Baldwin, and M. Shayegan, “Anisotropic two-dimensional disordered Wigner solid,” *Phys. Rev. Lett.* **129**, 036601 (2022).
 - 48 Y. P. Chen, G. Sambandamurthy, Z. H. Wang, R. M. Lewis, L. W. Engel, D. C. Tsui, P. D. Ye, L. N. Pfeiffer, and K. W. West, “Melting of a 2D quantum electron solid in high magnetic field,” *Nat. Phys.* **2**, 452–455 (2006).
 - 49 T. Knighton, Z. Wu, J. Huang, A. Serafin, J. S. Xia, L. N. Pfeiffer, and K. W. West, “Evidence of two-stage melting of Wigner solids,” *Phys. Rev. B* **97**, 085135 (2018).
 - 50 H. Deng, L. N. Pfeiffer, K. W. West, K. W. Baldwin, L. W. Engel, and M. Shayegan, “Probing the melting of a two-dimensional quantum Wigner crystal via its screening efficiency,” *Phys. Rev. Lett.* **122**, 116601 (2019).
 - 51 M. K. Ma, K. A. Villegas Rosales, H. Deng, Y. J. Chung, L. N. Pfeiffer, K. W. West, K. W. Baldwin, R. Winkler, and M. Shayegan, “Thermal and quantum melting phase diagrams for a magnetic-field-induced Wigner solid,” *Phys. Rev. Lett.* **125**, 036601 (2020).
 - 52 S. Kim, J. Bang, C. Lim, S. Y. Lee, J. Hyun, G. Lee, Y. Lee, J. D. Denlinger, S. Huh, C. Kim, S. Y. Song, J. Seo, D. Thapa, S.-G. Kim, Y. H. Lee, Y. Kim, and S. W. Kim, “Quantum electron liquid and its possible phase transition,” *Nature Mater.* **21**, 1269–1274 (2022).
 - 53 T. Smoleński, P. E. Dolgirev, C. Kuhlenskamp, A. Popert, Y. Shimazaki, P. Back, X. Lu, M. Kroner, K. Watanabe, T. Taniguchi, I. Esterlis, E. Demler, and A. Imamoglu, “Signatures of Wigner crystal of electrons in a monolayer semiconductor,” *Nature (London)* **595**, 53–57 (2021).
 - 54 Y. Xu, S. Liu, D. A. Rhodes, K. Watanabe, T. Taniguchi, J. Hone, V. Elser, K. F. Mak, and J. Shan, “Correlated insulating states at fractional fillings of moiré superlattices,” *Nature (London)* **587**, 214–218 (2020).
 - 55 H. Li, S. Li, E. C. Regan, D. Wang, W. Zhao, S. Kahn, K. Yumigeta, M. Blei, T. Taniguchi, K. Watanabe, S. Tongay, A. Zettl, M. F. Crommie, and F. Wang, “Imaging two-dimensional generalized Wigner crystals,” *Nature (London)* **597**, 650–654 (2021).
 - 56 Y. Zhou, J. Sung, E. Brutschea, I. Esterlis, Y. Wang, G. Scuri, R. J. Gelly, H. Heo, T. Taniguchi, K. Watanabe, G. Zaránd, M. D. Lukin, P. Kim, E. Demler, and H. Park, “Bilayer Wigner crystals in a transition metal dichalcogenide heterostructure,” *Nature (London)* **595**, 48–52 (2021).
 - 57 J. Falson, I. Sodemann, B. Skinner, D. Tabrea, Y. Kozuka, A. Tsukazaki, M. Kawasaki, K. von Klitzing, and J. H.

- Smet, “Competing correlated states around the zero-field Wigner crystallization transition of electrons in two dimensions,” *Nature Mater.* **21**, 311–316 (2022).
- ⁵⁸ C. Reichhardt, C. J. Olson, N. Grønbech-Jensen, and F. Nori, “Moving Wigner glasses and smectics: Dynamics of disordered Wigner crystals,” *Phys. Rev. Lett.* **86**, 4354–4357 (2001).
- ⁵⁹ C. Reichhardt and C. J. Olson Reichhardt, “Noise at the crossover from Wigner liquid to Wigner glass,” *Phys. Rev. Lett.* **93**, 176405 (2004).
- ⁶⁰ C. Reichhardt and C. J. O. Reichhardt, “Drive dependence of the Hall angle for a sliding Wigner crystal in a magnetic field,” *Phys. Rev. B* **103**, 125107 (2021).
- ⁶¹ C. Reichhardt and C. J. O. Reichhardt, “Nonlinear dynamics, avalanches and noise for driven Wigner crystals,” arXiv:2208.02929.
- ⁶² J. Lekner, “Summation of Coulomb fields in computer-simulated disordered-systems,” *Physica A* **176**, 485–498 (1991).
- ⁶³ N. Grønbech-Jensen, “Lekner summation of long range interactions in periodic systems,” *Int. J. Mod. Phys. C* **8**, 1287–1297 (1997).
- ⁶⁴ M.-C. Cha and H. A. Fertig, “Topological defects, orientational order, and depinning of the electron solid in a random potential,” *Phys. Rev. B* **50**, 14368–14380 (1994).